

## Capillary condensation in a square geometry with surface fields

M. Zubaszewska,<sup>1</sup> A. Gendiar,<sup>2</sup> and A. Drzewiński<sup>1</sup>

<sup>1</sup>*Institute of Physics, University of Zielona Góra, ulica Prof. Z. Szafrana 4a, 65-516 Zielona Góra, Poland*

<sup>2</sup>*Institute of Physics, Slovak Academy of Sciences, SK-845 11 Bratislava, Slovakia*

(Received 17 September 2012; published 12 December 2012; publisher error corrected 20 December 2012)

We study the influence of wetting on capillary condensation for a simple fluid in a square geometry with surface fields, where the reference system is an infinitely long slit. The corner transfer matrix renormalization group method has been extended to study a two-dimensional Ising model confined in an  $L \times L$  geometry with equal surface fields. Our results have confirmed that in both geometries the coexistence line shift is governed by the same scaling powers, but their prefactors are different.

DOI: [10.1103/PhysRevE.86.062104](https://doi.org/10.1103/PhysRevE.86.062104)

PACS number(s): 64.60.an, 64.60.De, 68.35.Rh, 05.10.—a

Porous materials are solids consisting of an interconnected network of pores. In recent years, microporous and mesoporous materials have been a focus of nanoscience and nanotechnology as their properties differ significantly from the same bulk materials [1,2]. Both the pore size and its shape, as well as the chemical nature of its surface, i.e., whether hydrophilic or hydrophobic, determine the properties of porous materials [3]. In a mesopore, the cumulative effect of the walls becomes important. After the formation of adsorbate layers of two to three molecular thickness on walls, further adsorption induces attractions between adsorbate molecules, leading to a sudden condensation of liquidlike adsorbate molecules inside the pores. This effect is analogous to the capillary condensation phenomenon [4].

The Ising square of a finite size  $L$  with the field  $h_1$  acting on all four surfaces (boundaries) can be used as an idealized representation of a simple fluid in a pore or between finely divided colloidal particles. The choice of the model entails the assumption that the intermolecular forces are short ranged in character; there are no dispersionlike forces. In fluid experiments the equivalent of the bulk magnetic field  $H$  describes the deviation of the critical chemical potential,  $H \sim \mu - \mu_0$ , that is determined by the density of the fluid in the reservoir. The phenomenon equivalent to the capillary condensation can be studied in magnetic systems [5]. Generally, in the bulk, phase coexistence occurs for temperatures  $T < T_c$  and for vanishing bulk magnetic field  $H$ . In a slit  $L \times \infty$  with identical surface fields at the boundaries, the combined effect of surface fields and confinement shifts the phase coexistence to a nonzero value of the bulk magnetic field  $H = H_{\text{coe}}(L)$ , which for large  $L$  scales as

$$H_{\text{coe}}(L) = \frac{\sigma_0 \cos \theta}{m_b} \frac{1}{L}, \quad (1)$$

where  $\sigma_0$ ,  $m_b$ , and  $\theta$  are the surface tension of the free up-spin–down-spin interface, bulk spontaneous magnetization, and contact angle given by Young’s equation, respectively [6]. In our case the liquid phase is represented by up-spins and the gas phase by down-spins, whereas area without spins is identified with the wall. The above equation is known in the literature as the Kelvin equation [7].

Wetting occurs in systems close to the line of phase coexistence when one phase may adsorb preferentially at a solid substrate. Typically, we model the substrate using a planar surface where the critical line  $h_w(T)$ , presented in Fig. 1, is

known exactly [8]:

$$\begin{aligned} & \exp(2J/k_B T) [\cosh(2J/k_B T) - \cosh(2h_w J/k_B T)] \\ & = \sinh(2J/k_B T). \end{aligned} \quad (2)$$

For this semi-infinite system if we approach the coexistence line from the gas side along a given isotherm ( $T_c > T > T_w$ ) the amount of liquid adsorbed on the surface  $l$  diverges:  $l \sim H^{-\beta_s^{\text{co}}}$ . Moreover, the phase transition, called the complete wetting, is characterized by the presence of the singular part of the excess surface free energy  $f_{\text{sing}} = H^{2-\alpha_s^{\text{co}}}$ . For the two-dimensional Ising model, the values of the critical exponents are  $2 - \alpha_s^{\text{co}} = 2/3$  and  $\beta_s^{\text{co}} = 1/3$ .

Consequently, when we consider the (pseudo-)two-dimensional Ising system in a slit geometry and the interaction between the liquid and walls is strong [above the  $h_w(T)$  line], the Kelvin equation fails and some corrections are necessary. The reason is that, although the macroscopically thick layer forms only for a semi-infinite system, a noticeable liquid layer intervenes between a gas and the wall for a finite-size system as well. Therefore, Foster pointed out [9] that if adsorbed layers were formed prior to condensation, the slit width  $L$  in Eq. (1) should be corrected by the layer thickness  $l$ . Derjaguin showed [10] that if solid-fluid forces decayed exponentially or had a finite range, the pore width  $L$  could be replaced by  $L - 2l$ .

Next, Evans *et al.* [4] showed that the effects of wetting layers were of quantitative rather than of qualitative importance for capillary condensation. Albano *et al.* [11] and Parry and Evans [12] analyzed the next-order correction term to the Kelvin equation for the semi-infinite system. Both studies, using scaling and thermodynamics arguments, concluded that for temperatures below the wetting temperature  $T_w$  (the dry regime) the leading correction to the scaling term was of type  $L^{-2}$ . Above the wetting (the wet regime) the correction is expected to be nonanalytic due to a singularity of the surface free energy. For the two-dimensional Ising model [11,12] the predicted correction term is proportional to  $L^{-5/3}$ .

In the subsequent numerical investigation, the density matrix renormalization techniques were employed [13,14]. For a large range of surface fields and temperature, higher-order corrections were not compatible with  $L^{-5/3}$ , but they were of type  $L^{-4/3}$ . It has been shown that this apparent disagreement was due to the fact that even for the large sizes considered

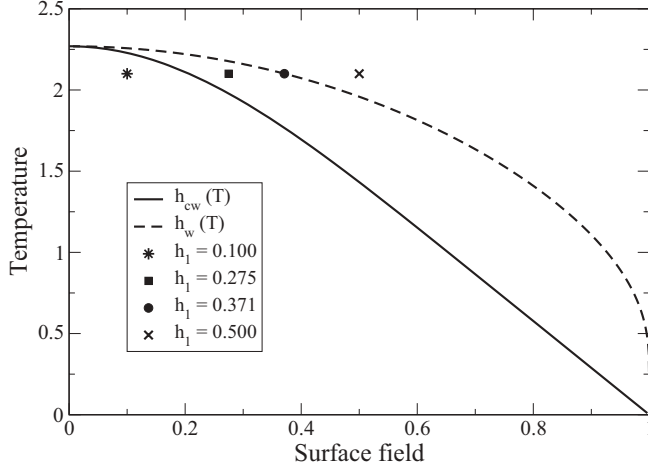


FIG. 1. The critical wetting lines for semi-infinite systems at  $T = 2.1$ : the corner wetting [ $h_{cw}(T)$ ] on the two planar surfaces forming a straight angle and wetting [ $h_w(T)$ ] on the planar surface. With respect to the planar wetting,  $h_1 = 0.1$  and  $0.275$  correspond to the dry regime, whereas  $h_1 = 0.371$  and  $0.5$  correspond to the wet one.

( $L \sim 150$ ) the wetting layer has a limited thickness, so that the singular part of the surface free energy that determines the correction-to-scaling behavior is dominated by the contacts with the walls.

In real systems, where properties of both pure fluids and fluid mixtures confined to nanoporous and microporous materials are under consideration [15], the squarelike geometry is more common than the slit one. In this case, the geometry of the system significantly affects the course of wetting phenomena because close to a corner the impact of the individual walls is strong, which should lead to more intensive formation of the wetting layer. Therefore, the corner wetting transition should also be taken into account [16,17]. As two sides of the square form the straight angle, the corresponding ( $L \rightarrow \infty$ ) corner wetting line  $h_{cw}(T)$ , presented in Fig. 1, is known exactly [18,19]:

$$\begin{aligned} & \cosh(2J/k_B T) - \exp(-2J/k_B T) \sinh^2(2J/k_B T) \\ &= \cosh(2Jh_{cw}/k_B T). \end{aligned} \quad (3)$$

To model the influence of wetting phenomena on the capillary condensation in a square geometry, we consider a square Ising ferromagnet subject to identical boundary fields with the following Hamiltonian:

$$\mathcal{H} = -J \left( \sum_{ijkl} S_{i,j} S_{k,\ell} - h_1 \sum_{\text{surface spins}} S_{i,j} - H \sum_{\text{all spins}} S_{i,j} \right), \quad (4)$$

with  $J > 0$  and  $S_{i,j} = \pm 1$ . The first sum is taken over the nearest neighbors, while the second sum is performed on spins at the surface only. The surface field  $h_1$  corresponding to direct short-range interactions between the walls and spins is related to the preferential adsorption on the surface for one of the two phases. The uniform bulk magnetic field  $H$  acts over all spins.

The origin of applied numerical method, called the corner transfer matrix renormalization group (CTMRG), came from Baxter [20]. Next Nishino and Okunishi [21] combined his

corner transfer matrix method with the ideas from the density matrix renormalization group (DMRG) method approach. The last technique was developed by White [22,23] for the study of ground-state properties of quantum spin chains and next extended by Nishino to two-dimensional classical systems in a slit geometry [24].

The general idea is to find a representation of the configurational space in a restricted space that is much smaller than the original one:  $m \ll 2^{L^2}$ . This truncation is done through the construction of a reduced density matrix whose eigenstates provide the optimal basis set  $m$ . Of course, the larger  $m$ , the better accuracy, so in the present case we keep this parameter up to  $m = 400$ .

Although in the original CTMRG algorithm the full transfer matrix is never constructed, we have modified it to determine the two eigenvectors related to the largest eigenvalues. Because each of these vectors dominates on the opposite side of the coexistence line, using both vectors for the construction of the density matrix guarantees that the Hamiltonian is properly projected on the subspace of most probable states. Our results have not shown any ambiguities of the calculated free energy and, by increasing the number of states kept  $m$ , our results (the free energy) converged. To have a point of reference, we compared the results for the square geometry with the results for the slit geometry, where the DMRG technique was applied [13,14].

Owing to the finiteness of  $L$  and to the nonvanishing surface field  $h_1$  the (pseudo)coexistence lines (for both geometries) are shifted with respect to the bulk coexistence line ( $H = 0$ ). As one can see in Fig. 2 this effect is much stronger for the squarelike system. This is easy to understand if one remembers that the influence of walls on the individual spins is here reinforced with respect to the slit geometry.

A schematic drawing of the fluid shape adopted in a square geometry below ( $h_1 = 0.1$ ) and above ( $h_1 = 0.6$ ) wetting is demonstrated in Fig. 3. Both top magnetization profiles correspond to the phase when a liquid fills the squarelike pore. For a weak field the magnetization is lower near walls, whereas for a strong field the magnetization is essentially uniformly

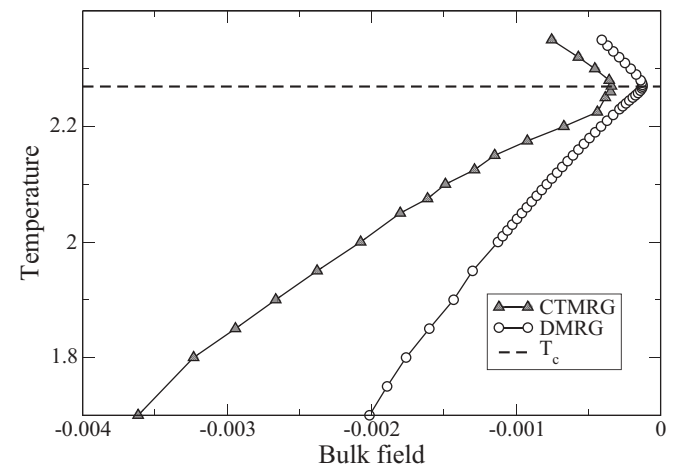


FIG. 2. Pseudocoexistence lines for the square (triangles) and slit (circles) systems for  $L = 500$  and  $h_1 = 0.8$ .  $L$  is measured in units of lattice constant, whereas  $h_1$  is in  $J$  units.

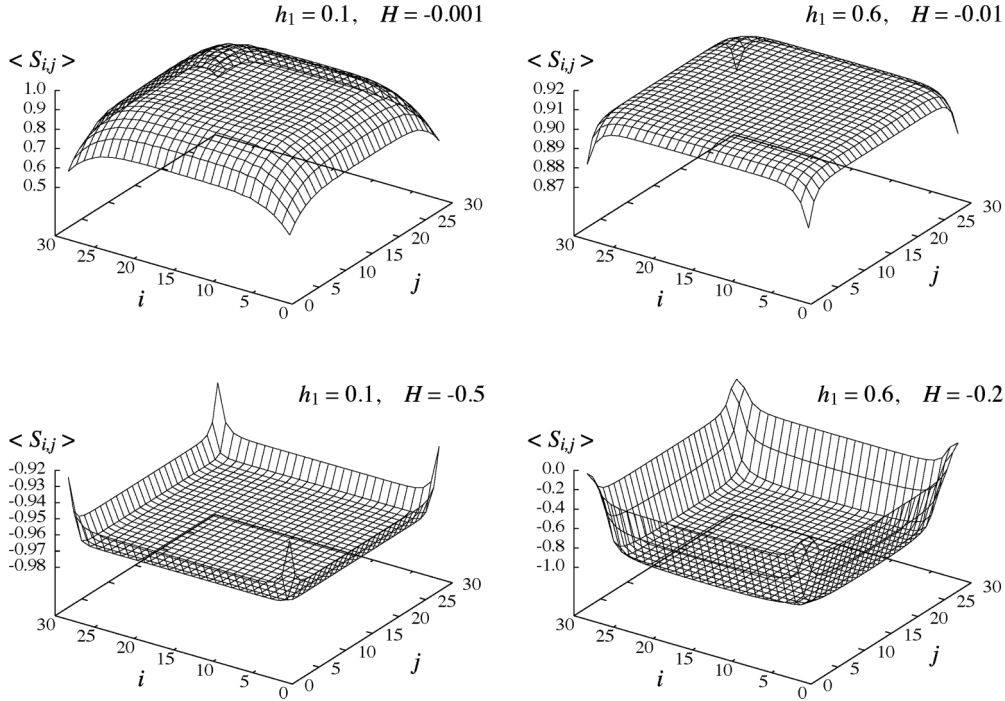


FIG. 3. Two-dimensional magnetization profiles  $\langle s_{i,j} \rangle$  on the square geometry  $31 \times 31$  for the two values of the surface field  $h_1 = 0.1$  (left-hand graphs) and  $h_1 = 0.6$  (right-hand graphs) calculated at fixed temperature  $T = 2.0$ . The profiles change their shapes and spin polarizations while varying the bulk field value  $H$  below and above the wetting temperature  $T_w(h_1 = 0.1) = 2.257$  and  $T_w(h_1 = 0.6) = 1.814$ , respectively.

high throughout the square. The bottom magnetization profiles illustrate the situation on the other side of the coexistence line, when the gas phase occupies the middle of the square. While the weak-field magnetization profile only slightly increases at the square edges, the strong-field magnetization profile increases considerably, which corresponds to creation of the liquid layer. Note that the surface impact is always enhanced in the square corners, although limited to a relatively small area.

The real phase transition (the complete wetting) occurs only in a semi-infinite system. Since we deal with a finite-size system, the thickness of the wetting layer is limited, and a sharp liquid-gas interface is not observed. Furthermore, because for a weak surface field (below the wetting line) there remains a thin liquid layer between a gas and the wall, the gas-wall interface formally never occurs. For the same reason, below the wetting line the isolated droplets of liquid cannot be observed on the wall, so the contact angle cannot be drawn.

As a useful tool for the analysis of the higher terms of the Kelvin equation, we introduce the logarithmic derivative which acts as an effective dominant exponent,

$$\alpha(L) = -\frac{\ln[H_{\text{coe}}(L + \Delta L)] - \ln[H_{\text{coe}}(L)]}{\ln(L + \Delta L) - \ln(L)}. \quad (5)$$

When the following expansion of the Kelvin equation is assumed,

$$H_{\text{coe}} = \frac{A}{L^\alpha} + \frac{B}{L^\gamma}, \quad (6)$$

combining both formulas, we obtain the first-order expansion for the effective exponent,

$$\alpha(L) = \alpha + (\gamma - \alpha) \frac{B}{A} \frac{1}{L^{\gamma-\alpha}}. \quad (7)$$

The Kelvin equation is expected to be valid to the first order for all  $T < T_c$ , but since only a limited size  $L$  is available for the numerical computation, it is preferable to consider only temperatures not too close to the bulk critical temperature, where the scaling of the capillary critical point  $H_{\text{crit}}(L) \sim L^{15/8}$  is present [6]. Therefore, our results refer to temperature  $T = 2.1$ , but we have checked that they do not qualitatively change for other temperatures.

Figure 4 shows that for a wide range of the surface fields, when the system grows, the value  $\alpha(L)$  goes to  $\alpha = 1$ . It confirms that, to the accuracy of the first-order expansion, the shift of the phase coexistence and the system size are reciprocal in both geometries.

For the wet phase ( $\theta = 0$ ) in the slit geometry, the exact formula for the coefficient is known [see Eq. (1)], giving  $A(T = 2.1) = 0.335$  which very well agrees with our estimated value 0.345. Generally, our numerical fittings for curves  $H_{\text{coe}}(L)$  according to Eq. (6) show that the ratio of the main prefactors for the slit and square geometries is  $A_{\text{slit}}/A_{\text{square}} \sim 1/2$  for each value of the surface field. For example, below the wetting  $A_{\text{slit}}(h_1 = 0.1) = 0.121$  and  $A_{\text{square}}(h_1 = 0.1) = 0.242$ , whereas above the wetting  $A_{\text{slit}}(h_1 = 0.5) = 0.345$  and  $A_{\text{square}}(h_1 = 0.5) = 0.669$ . This fact can be explained in the following way: when the size of the square increases, the impact of the corners remains more or less the same, but the influence of the sides increases. Thus, when  $L$  goes to infinity,

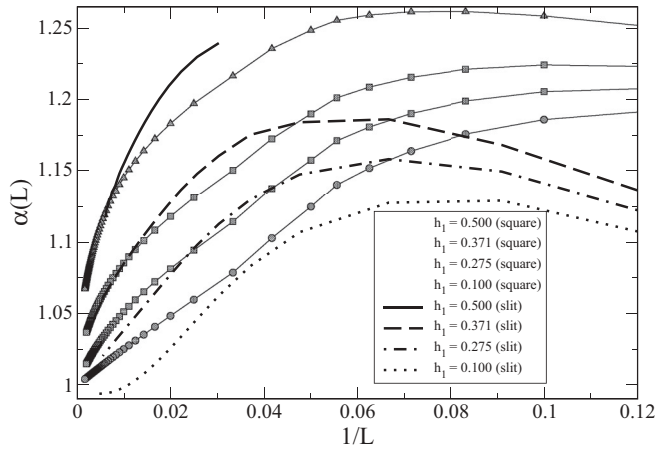


FIG. 4. Plots of the local exponent for both geometries at  $T = 2.1$ . Lines correspond to the square geometry, whereas the symbols are related to the slit one.

the system begins to resemble a set of two slits perpendicular to each other.

As one can see in Figs. 4 and 5, the shape of the curves indicates that we are dealing with various expressions of a higher order. First of all, the  $B$  coefficient, which is always positive in the slit geometry, is negative in the dry regime for the square geometry. This is manifested by the  $\alpha(L)$  function minima for small  $1/L$ , where the leading correction  $B/L^\nu$  dominates. Obviously, the next correction has to be positive. Moreover, in the wet regime, where the  $B$  coefficients are positive, as one can see in Fig. 4, the curves corresponding to the same value of the surface field start to overlap when  $L$  becomes enough large.

In the square geometry, as far as the leading correction terms are concerned, the precise analysis of our numerical results shows, in both the dry and wet regimes, they are the same as in the slit geometry (see Fig. 5).

It is worth adding that the values of the surface field  $h_1 = 0.1$  ( $h_1 = 0.5$ ) were chosen to be in the dry (wet) regime with respect to both wetting curves (see Fig. 1). Although the presented curves correspond to infinite systems, we are dealing with systems large enough to guarantee that both points are localized on the appropriate side of the wetting curves.

To sum up, the corner transfer matrix renormalization group method has been extended to study the equilibrium statistical mechanics of simple fluids confined in the square geometry, providing some input for understanding experiments in porous materials. As the method is not perturbative, it can be applied to arbitrary values of the model parameters and yields accurate results, provided that a convergence of the free energy is reached. Accuracy of the CTMRG method is completely controlled by varying the number of the states kept. Moreover,

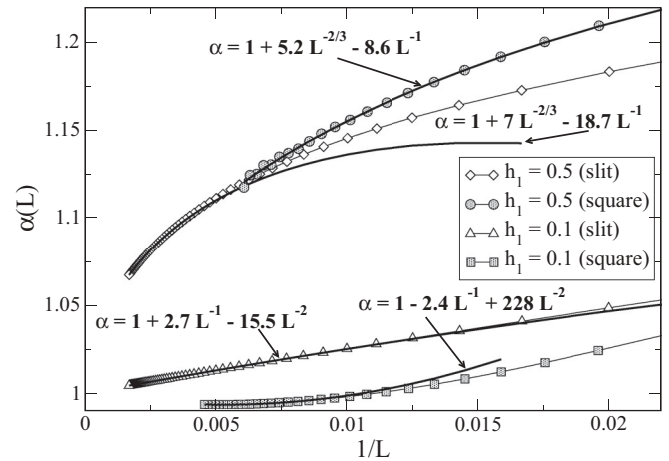


FIG. 5. The effective exponents  $\alpha(L)$  and their fitting curves denoted by the thick lines for two sample values of the surface field:  $h_1 = 0.1$  for the dry system and  $h_1 = 0.5$  for the wet system [see Fig. (1)].

the method does not suffer from getting stuck in a local minimum of the free energy instead of the true global free energy minimum, which is a typical problem in Monte Carlo simulations. There are neither metastabilities nor hysteresis effects provided that  $m$  is set to be sufficiently large, which is our case concluded by the converged free energy.

Our results confirm that in a more realistic (square) geometry the coexistence line shift is inversely proportional to the system size  $L$  and the main prefactor is two times larger than for the case of an infinitely long slit of width  $L$ . Moreover, for the square geometry the leading correction term to the Kelvin equation becomes negative in the dry regime.

We have also found that similarly to the slit geometry the leading corrections to scaling in the square geometry are of type  $1/L^2$  in the dry regime and of type  $1/L^{5/3}$  in the wet regime. The last correction is again nonanalytic due to a singularity of the surface free energy.

Curve fitting was carried out for the values of the surface fields that correspond to the dry or wet regime with respect to both wetting lines defined by Eqs. (2) and (3). The area between the wetting lines was not analyzed in detail, although the strongest competition can be expected between the two types of wetting. This requires an examination of larger systems, which implies the need for a more precise calculation. In our next studies, we aim to increase the precision of the numerical results by additional improvement of the CTMRG algorithm.

This work was done under Projects No. VEGA-2/0074/12, No. APVV-0646010 (COQI), and No. POKL.04.01.01-00-041/09-00. Numerical calculations were performed in WCSS Wrocław (Poland, Grant No. 82).

- [1] J. N. Israelachvili, *Intermolecular and Surface Forces*, 2nd ed. (Academic Press, New York, 1992).  
 [2] *Handbook of Nanophysics: Functional Nanomaterials*, edited by Klaus D. Sattler (Taylor & Francis, Boca Raton, FL, 2011).

- [3] Lev D. Gelb, K. E. Gubbins, R. Radhakrishnan, and M. Sliwinski-Bartkowiak, *Rep. Prog. Phys.* **62**, 1573 (1999).  
 [4] R. Evans, U. Marini Bettolo Marconi, and P. Tarazona, *J. Chem. Phys.* **84**, 2376 (1986).



- [5] K. Binder and D. Landau, *J. Chem. Phys.* **96**, 1444 (1992); K. Binder, D. Landau, and M. Müller, *J. Stat. Phys.* **110**, 1411 (2003).
- [6] M. E. Fisher and H. Nakanishi, *J. Chem. Phys.* **75**, 5857 (1981); H. Nakanishi and M. E. Fisher, *ibid.* **78**, 3279 (1983).
- [7] W. Thomson, *Philos. Mag.* **42**, 448 (1871).
- [8] D. B. Abraham, *Phys. Rev. Lett.* **44**, 1165 (1980).
- [9] A. G. Foster, *Trans. Faraday Soc.* **28**, 645 (1932).
- [10] B. V. Derjaguin, *Zh. Fiz. Khim.* **14**, 137 (1940).
- [11] E. V. Albano, K. Binder, D. W. Heermann, and W. Paul, *J. Chem. Phys.* **91**, 3700 (1989).
- [12] A. O. Parry and R. Evans, *J. Phys. A* **25**, 275 (1992).
- [13] E. Carlon, A. Drzewiński, and J. Rogiers, *Phys. Rev. B* **58**, 5070 (1998).
- [14] A. Drzewiński and K. Szota, *Phys. Rev. E* **71**, 056110 (2005).
- [15] I. Brovchenko and A. Oleinikova, *Interfacial and Confined Water* (Elsevier, Amsterdam, 2008).
- [16] A. O. Parry, A. J. Wood, and C. Rascón, *J. Phys.: Condens. Matter* **12**, 7671 (2000); M. J. Greenall, A. O. Parry, and J. M. Romero-Enrique, *ibid.* **16**, 2515 (2004).
- [17] A. Milchev, M. Müller, K. Binder, and D. P. Landau, *Phys. Rev. E* **68**, 031601 (2003); A. Milchev, A. De Virgiliis, and K. Binder, *J. Phys.: Condens. Matter* **17**, 6783 (2005).
- [18] A. O. Parry, A. J. Wood, E. Carlon, and A. Drzewinski, *Phys. Rev. Lett.* **87**, 196103 (2001).
- [19] D. B. Abraham and A. Maciolek, *Phys. Rev. Lett.* **89**, 286101 (2002).
- [20] R. J. Baxter, *J. Stat. Phys.* **19**, 461 (1978).
- [21] T. Nishino and K. Okunishi, *J. Phys. Soc. Jpn.* **65**, 891 (1996); K. Ueda, R. Krčmár, A. Gendiar, and T. Nishino, *ibid.* **76**, 084004 (2007).
- [22] S. R. White, *Phys. Rev. Lett.* **69**, 2863 (1992); *Phys. Rev. B* **48**, 10345 (1993).
- [23] U. Schollwoeck, *Rev. Mod. Phys.* **77**, 259 (2005); K. Hallberg, *Adv. Phys.* **55**, 477 (2006); U. Schollwoeck, *Ann. Phys. (NY)* **326**, 96 (2011).
- [24] T. Nishino, *J. Phys. Soc. Jpn.* **64**, 3598 (1995).